SYMMETRY ASPECTS OF FISSION FRAGMENT MASS DISTRIBUTION IN ^{238}U(^{18}O,F) REACTION

ASPECTOS DE SIMETRÍA DE LA DISTRIBUCIÓN MASIVA DEL FRAGMENTO DE FISIÓN EN ^{238}U(^{18}O,F) REACCIÓN

R. Gupta†

Department of Physics, Swami Swatantranand Memorial College, India. rajivguptamirage@gmail.com†
† corresponding author

Recibido 25/1/2020; Aceptado 5/6/2020

Fine structure dips in the fission fragment mass distribution in $^{238}U(^{18}O, f)$ reaction arise mainly due to breakdown of the spin-isospin symmetry. The average proton-neutron interaction for each decay mode is calculated by using double differences of binding energies, It is shown that its decreasing trend at N=82 has direct relevance with the breakdown of spin-isospin symmetry. The maxima in the p-n interaction correspond to partial restoration of spin-isospin symmetry and therefore, help in limiting the number of neutrons evaporated in each decay channel. Also, calculations based on the asymmetric two-center shell model explain not only the observed mass distribution nicely but suggests a possible value of extending these experiments beyond their present mass limits.

Las protuberancias en la estructura fina observada en la distribución de masa para la reacción $^{238}U(^{18}O, f)$ obedece, principalmente, a la ruptura de simetría spin-isospin. La interacción promedio entre el proton y el neutrón para cada modo de decaimiento se calcula utilizando diferencias dobles de las energías de enlace. Se demuestra que la tendencia decreciente con $N = 82$ tiene un vínculo directo con la ruptura de la simetría spin-isospin. Los máximos en la interacción $p - n$ corresponden a la restauración parcial de la simetría spin-isospin, lo cual contribuye a limitar el número de neutrones evaporados en cada canal de decaimiento. Adicionalmente, los cálculos basados en el modelo de dos centros explican elegantemente no solo la distribución de masa sino también sugieren un posible valor para extender estos experimentos más allá de los límites de masa actuales.

PACS: Shell model (modelo de capas), 21.60.Cs; compound nucleus (núcleos compuestos), 25.70.Gh; fission process (procesos de fisión), 24.75.+i; nuclear reactions (reacciones nucleares), 24.10.-i

I. INTRODUCTION

In the reaction of 100 MeV ^{18}O beam bombarded on the ^{238}U target recently, the cross-section for making the fused system is measured and this fused system is found to disintegrate with fragment mass distribution centered around zero mass asymmetry [1]. The measured excitation energy is about 60 % of the Coulomb barrier height. The observed spectrum shows fine structure dips corresponding to mass numbers A=112 and 124 plus their complementary fragment masses. The authors in Ref. [1] claim that these dips refer to the closed shell nuclei.

This signature of the fission fragment mass distribution has opened up a new era for understanding the shell closure at large $\frac{N}{Z}$ ratios. Here, N and Z refers to neutron number and proton number, respectively. So far the confirmation of shell closure and magic numbers were evidenced usually by using one of the following experimental approaches:

(i) Study of masses and separation energies;

(ii) Determination of energies of the first excited state ($E2$) of even-even nuclei;

(iii) The reduced transition probability $B(E2; 0^+ \rightarrow 2^+)$ value along an isotopic chain of proton-magic nuclei, provides a sensitive signature of shell evolution.

In this paper, one show that the observed dips in the mass distribution arise mainly due to breakdown of the spin-isospin symmetry. In addition to the empirical estimates, asymmetric two-center shell model (ATCSM) [2–4] based calculations have also been performed to justify the observed mass distribution.

II. INTERACTION ENERGY BETWEEN N-P PAIRS

Firstly, we try to understand the observed structure in the fission fragment mass distribution by using the interaction energy between n-p pairs. Experimental binding energies ($B(Z,N)$) [5] generally represents the sum of all these nucleonic interactions. For even-even nuclei, the average p-n interaction of last nucleons can be extracted from the double differences of binding energies [6,7] and is written as [8,9],

$$\delta V_{pn}(Z,N) = \frac{1}{4}\Big[[B(Z,N) - B(Z,N-2)] - [B(Z-2,N) - B(Z-2,N-2)]\Big] \quad (1)$$

Here, a given $\delta V_{pn}(Z,N)$ value for even-even nuclei refers to the interaction of the (Z-1) and Zth protons with the (N-1) and Nth neutrons.

Here, $\delta V_{pn}(Z,N)$ interactions for all the observed even-even isotopes (as shown in figure 2 of Ref. [1]), namely, $^{90-96}Sr$, $^{96-102}Zr$, $^{98-108}Mo$, $^{104-112}Ru$, $^{108-116}Pd$, $^{114-122}Cd$, $^{116-128}Sn$,

$^{124-134}Te$, $^{130-138}Xe$, $^{136-144}Ba$, $^{142-148}Ce$, $^{146-152}Nd$ and $^{150-158}Sm$ have been calculated and are plotted as a function of neutron number N in figure 1 1. A remarkable outcome of this plot is that for nuclei lying between $52 \leq Z \leq 56$ with N=82, a sharp dip occurs in each of these isotones. These sharp minima in semi-magic nuclei refer to weak strength of their $\delta V_{pn}(Z,N)$ interaction and arise mainly due to breakdown of the spin-isospin symmetry as discussed below.

Recently, Cakirli et al. [10] have proposed an intuitive method to understand the variation of δV_{pn} interaction from the orbital overlap of protons and neutrons. Following their procedure, one has analyzed the strength of p-n interaction by using the ordering of single particle levels. Single particle levels of protons and neutrons for $^{138}_{56}Ba$ have also been shown specifically in table 1 by using the Wood-Saxon potential. In this table, the highest filled shells and the lowest empty shells are also listed, together with the energy gap between filled and unfilled shells. The spacing between shells are measured from the shell closest to the Fermi surface. In this table, the results for $^{208}_{82}Pb$ nucleus are also shown for comparison. It is quite evident from table 1 that in case of $^{208}_{82}Pb$, both types of nucleons (proton and neutron) occupy low j orbitals. The overlapping between these orbitals is significantly large and hence gives a strong δV_{pn} value as suggested in Ref. [10]. Whereas in case of $^{138}_{56}Ba$, the protons in high j orbitals overlap poorly with the neutrons in low j orbits and therefore, results in smaller p-n interaction.

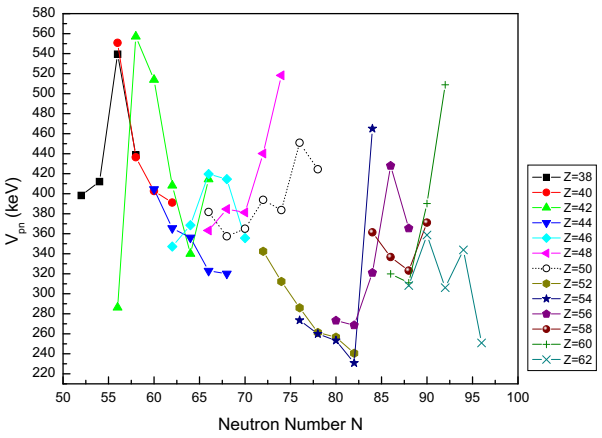

Figure 1. The proton-neutron interaction $\delta V_{pn}(Z,N)$ vs.the neutron number N.

Table 1. The ordering of single particle levels.Here, the energies are measured in MeV

Nucleus	Filled shells	Gap	Empty shells
$^{138}_{56}Ba$	$g_{\frac{9}{2}}\ d_{\frac{5}{2}}$	0.8(p)	$g_{\frac{7}{2}}\ d_{\frac{3}{2}}\ s_{\frac{1}{2}}$
$^{138}_{56}Ba$	$s_{\frac{1}{2}}\ d_{\frac{3}{2}}\ h_{\frac{11}{2}}$	4.7(n)	$f_{\frac{7}{2}}\ p_{\frac{3}{2}}\ h_{\frac{9}{2}}\ p_{\frac{1}{2}}\ f_{\frac{5}{2}}$
$^{208}_{82}Pb$	$g_{\frac{7}{2}}\ d_{\frac{5}{2}}\ h_{\frac{11}{2}}\ d_{\frac{3}{2}}\ s_{\frac{1}{2}}$	3.1(p)	$h_{\frac{9}{2}}\ f_{\frac{7}{2}}\ i_{\frac{13}{2}}\ f_{\frac{5}{2}}$
$^{208}_{82}Pb$	$i_{\frac{13}{2}}\ f_{\frac{5}{2}}\ p_{\frac{1}{2}}$	3.4(n)	$g_{\frac{9}{2}}\ i_{\frac{11}{2}}\ j_{\frac{15}{2}}\ d_{\frac{5}{2}}\ g_{\frac{7}{2}}$

Further, it is also noticed from this Table that in case of $^{138}_{56}Ba$, the neutron gap between filled and unfilled shells is sufficiently large (~4.7 MeV) as compare to that of proton gap (~0.8 MeV). Whereas in case of $^{208}_{82}Pb$, nearly same shell gaps emerge for both the nucleons. For the doubly closed shells with T_0 ($=\frac{N-Z}{2}$) $\neq 0$ as in the case of $^{208}_{82}Pb$, the higher-lying proton and neutron hole configurations give rise to an isospin doublet with $T = T_0 \pm \frac{1}{2}$. The separation energy is given, to a first approximation, by [11]

$$\begin{aligned}\delta E &= E(T = T_0 + \frac{1}{2}) - E(T = T_0 - \frac{1}{2}) \\ &= \frac{T_0 + \frac{1}{2}}{A} < lj|V_1(r)|lj >\end{aligned} \tag{2}$$

in terms of the radial matrix element of the isovector potential $V_1(r)$. An additional effect may arise from the isovector part of the spin-orbit coupling in the nuclear potential. The empirical evidence of the separation between isospin doublets for single particle configuration is found to imply a strength of the isovector potential. It is quite large in case of $^{208}_{82}Pb$. On the other hand in case of $^{138}_{56}Ba$, the state that is obtained by transforming one of the $2T_0$ excess neutrons into a proton has less pairing gap. Therefore, implies a weak strength of the isovector potential.

III. RESULTS AND DISCUSSION

Both these factors i.e., (i) a poor overlaps of proton and neutron orbitals and (ii) small gap between filled and unfilled shells of protons fully support the minimum strength of δV_{pn} in three isotones ($_{52}Te$, $_{54}Xe$ and $_{56}Ba$) as shown in figure 1.

Recently, Van Isacker et al. [8] have established that the large value of δV_{pn} for N=Z nuclei fulfills spin-isospin symmetry. One conclude from the above observations that a large overlap between the orbitals and nearly same shell gaps in both the nucleons ensure to restore the spin-isospin symmetry partially. This symmetry is badly broken if these orbitals overlap poorly and their shell gaps are quite different as remarked in the case of three isotones in figure 1. Thus the breakdown of spin-isospin symmetry leads to reduced mass yields of the fragments $^{134}_{52}Te$, $^{136}_{54}Xe$ and $^{138}_{56}Ba$. Accordingly, the production of their complementary fragments (A ~112) are also less.

It is worthwhile to mention here that the maxima in figure 1 refers to partial restoration of spin-isospin symmetry. The major advantage of this symmetry is that one can estimate the number of neutrons emitted in each channel as follows $^{256}_{100}Fm \rightarrow {}^{A_1}_{Z_1}X + {}^{A_2}_{Z_2}Y + p_0^1 n$, with $Z_1 + Z_2$=100. Here, X and Y refer to fission fragment and its complementary partner corresponding to maxima. From this analysis it is found that $8 \leq p \leq 10$, which is in good agreement with the observed neutron emission limit [1].

In order to understand the dip in the spectrum corresponding to $^{124}_{50}Sn$, the ratio of excitation energies of the first 4^+ and the first 2^+ excited states of the observed fission fragments has been plotted in figure 2. This ratio is an appropriate measure of collectivity in nuclei. It is evident that the collectivity ceases sharply for nuclei $^{134}_{52}Te$, $^{136}_{54}Xe$ and $^{138}_{56}Ba$. This implies that these isotones have been driven towards the spherical shape by neutron magicity. Similarly, the observed isotopes corresponding to Z=50 have nearly constant ratio and its value is less than 2. Also, a shallow minimum is

observed in figure 1 at $^{124}_{50}Sn$. These observations reveal that in the composite system, the partner having closed shell configuration cannot be easily deformed, only the complementary partner has to attain larger deformation for moving toward the scission configuration. Hence, in the fission fragment mass distribution, the yield corresponding to these mass channels is reduced significantly.

In order to explain the complete structure in mass distribution, calculations has been carried out by using the ATCSM in which isospin effects are included. Since the observed fission occurs below the Coulomb barrier, therefore, the average number of neutrons emitted per fission is taken to be nearly 2. So, one has considered the fission of $^{254}_{100}Fm$ instead of $^{256}_{100}Fm$ [12].

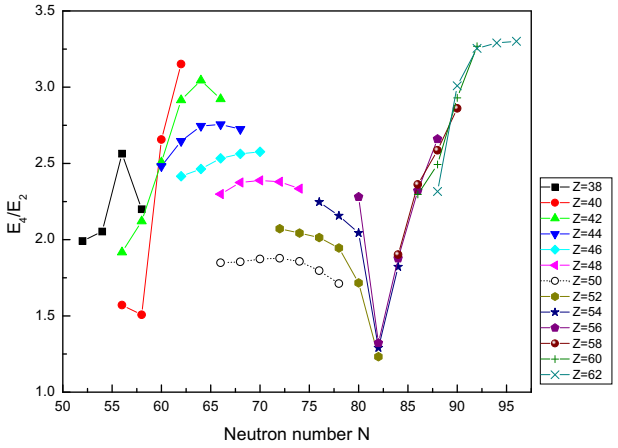

Figure 2. The ratio $\frac{E_4}{E_2}$ vs. the neutron number N.

Using the coordinates of relative separation R, the deformations β_i (i=1,2), the neck parameter ϵ, the mass asymmetry η=$\frac{A_1-A_2}{A_1+A_2}$, and the charge asymmetry η_Z=$\frac{Z_1-Z_2}{Z_1+Z_2}$, the collective Hamiltonian of the fragmentation theory [13] is written as

$$H = T(R, \beta_i, \eta, \eta_Z; \dot{R}, \dot{\beta}_i, \dot{\eta}, \dot{\eta_Z}) + V(R, \beta_i, \eta, \eta_Z), \quad (3)$$

where the collective potential V is calculated by using the Strutinsky method from the ATCSM [14] and the appropriate liquid drop model (LDM) [15]. It is given by

$$V(\eta) = V_{LDM} + \delta u + \delta p, \quad (4)$$

where δu and δp are the shell and the pairing contributions, respectively. For $R < R_1 + R_2$, the adiabatic potentials are obtained by carrying out three dimensional minimization in shape parameters β_i and ϵ and, for R=$R_1 + R_2$, the potential can be expressed simply as

$$V(\eta)\,|_{R_1+R_2} = -B_1(A_1, Z_1) - B_2(A_2, Z_2) + E_C. \quad (5)$$

The three dimensional (β_i and ϵ) calculations of the ATCSM potential (equation (3)) for every set of R, η and η_Z involve lot of computational volume. This severe problem has been overcome with suitable simplifications as discussed below.

Since, the fission fragment mass and charge distributions are decided during saddle to scission configuration and are related to scission configuration (i.e., $R_1 + R_2$), therefore, the charges Z_1 and Z_2 of the fission fragments are fixed by minimizing the sum of the experimental binding energies, $B_i(i = 1, 2)$ (taken in terms of mass excess from Ref. [5]) and the Coulomb energy $E_C = \frac{Z_1 Z_2 e^2}{R_1+R_2}$ as discussed in equation (5). In these calculations, mass asymmetry η has been varied in step of two-nucleon transfer (i.e., $\Delta\eta$=$\frac{2}{A}$).

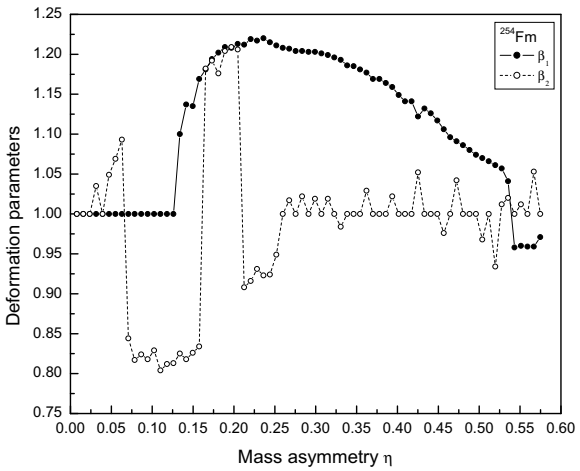

Figure 3. The asymptotic deformation parameters as a function of η. The deformation parameters are taken from [16].

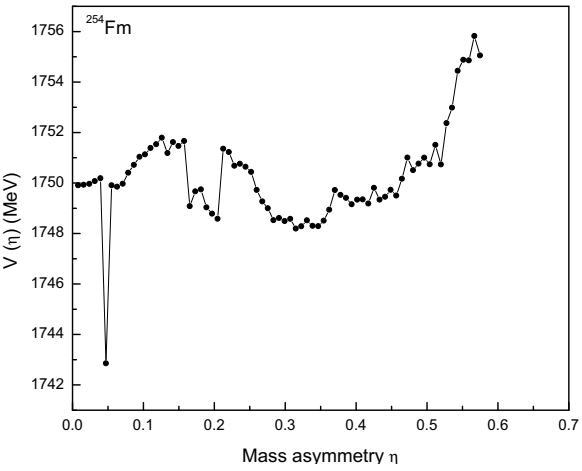

Figure 4. The ATCSM potential, $V(\eta)$ vs. η.

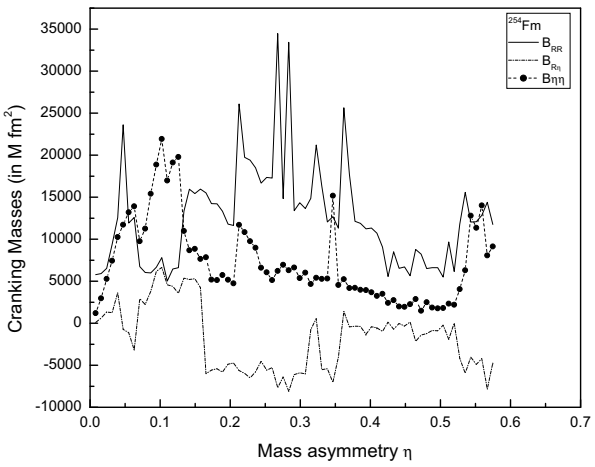

Figure 5. The cranking masses vs. η.

Thus knowing the fission fragments at the scission configuration, one has taken their deformation parameters β_i (i=1,2) from Seeger [16] and are shown in figure 3 vs. the mass asymmetry. Finally, ϵ is fixed by minimizing potential energy in equation (4) at $R_1 + R_2$=12.6fm. This minimized potential $V(\eta)$ vs. the mass asymmetry is shown in figure 4.

The mass parameters B_{ij} (i and j=η and R) for the kinetic energy term are consistently calculated by using the ATCSM states in the cranking formula based on the BCS formalism (see Refs. [17] and [18]) and are shown in figure 5. Here, following the work of Greiner and Collaborators [19, 20], it is shown in this plot (figure 5) that the cranking coupling masses $B_{R\eta}$(dash-dotted curve) are very small such that $B_{R\eta} \ll \sqrt{B_{RR}B_{\eta\eta}}$ hold good. Also, this inequality is confirmed explicitly from the plots of masses B_{RR}, $B_{\eta\eta}$ and $B_{R\eta}$ (see Ref. [21]). Furthermore, an experimental support for this assumption is also given in Ref. [22]. Also, it has been shown by Gupta and co-workers [23, 24] that the coupling effects of relative motion (R) to mass asymmetry (η) coordinates in the potential are very small for fission charge distributions and α-particle transfer resonances. In view of these results, R and η degrees of freedom have been treated in a decoupled mode [25].

Finally, for the dynamical mass fragmentation process, we quantize the motion in the mass asymmetry coordinate η. Considering that the η motion is fast compared to the R motion, R can be taken as a time-independent parameter and the stationary Schrodinger equation in η can be written as using the Pauli-Padolsky prescription [17],

$$\Big[-\frac{\hbar^2}{2\sqrt{B_{\eta\eta}}}\frac{\partial}{\partial\eta}\Big(\frac{1}{\sqrt{B_{\eta\eta}}}\frac{\partial}{\partial\eta}\Big) + V(\eta)\Big]\psi^{\nu}(\eta) = E_{\eta}{}^{\nu}\psi^{\nu}(\eta). \quad (6)$$

We have chosen the value of constant R at a point just near the scission configuration. Here, the quantum number ν=0,1,2,... counts the vibrational states ψ^{ν} in the potential.

Knowing the potential and the cranking masses, respectively, from figure 4 and figure 5 (dotted line with points) equation (6) is numerically solved. Then, $|\psi(\eta)|^2$ gives the probability of finding the mass fragmentation η at $R_1 + R_2$ (=12.6fm) and with fixed η_Z on the decay path, which on normalization gives the mass distribution yield

$$Y = |\psi(\eta)|^2\sqrt{B_{\eta\eta}}\frac{4}{A}. \quad (7)$$

Here, the normalization is numerically checked. This yield is directly comparable with experiments. If only the ground state contributes then ν=0. However, if the system is excited or we allow the effects of interaction with other degrees of freedom, the higher values of ν would contribute. The possible consequences of such excitations are also included through the simple Boltzmann-like occupation of excited state

$$|\psi(\eta)|^2 = \frac{\sum_{\nu}|\psi^{\nu}|^2\exp\Big(-\frac{E^{\nu}}{\Theta}\Big)}{\sum_{\nu}\exp(-\frac{E^{\nu}}{\Theta})} \quad (8)$$

It should be noted that Θ is the nuclear temperature (in MeV) and is related to the excitation energy E^* by the following statistical expression [26]

$$\Theta = \sqrt{\frac{10E^*}{A}}. \quad (9)$$

Here, the level density parameter is taken as $\frac{A}{10}$. However, it should be noted that the level density parameters containing phenomenological parameterizations based on the modified Fermi gas, superfluid models and realistic microscopic calculations of single-particle level scheme with energy, spin, parity and shell correction dependencies may further improve the results [27–29]

The normalized yield as a function of mass number A on a semilogarithmic scale is shown in figure 6 by solid curve with points. In this plot dotted curve refers to the yield by using the ATCSM potential (figure 4) with average mass parameter ($B_{\eta\eta}$= 0.7×10$^4 Mfm^2$). It is obvious from this plot that the solid curve with points reproduces the dips at fission fragments ^{112}Ru +^{142} Ba and ^{126}Sn +^{128} Sn and are in close resemblance with the observed data [1].

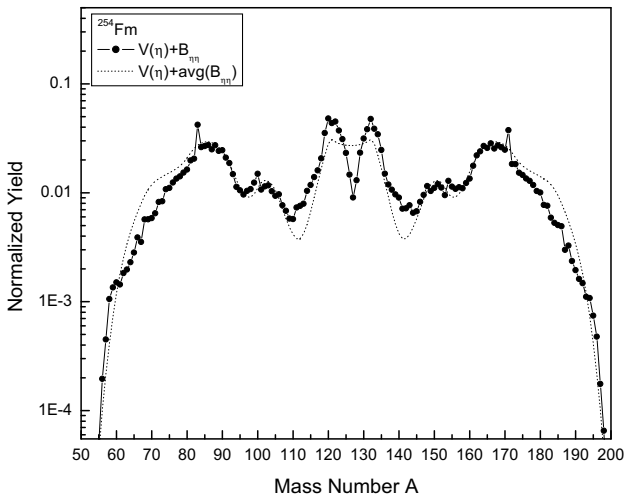

Figure 6. The normalized yield as a function of A for the fissioning nucleus ^{254}Fm by using the ATCSM potential and cranking masses (solid line with points). The dotted line refers to yield with the ATCSM potential and average mass.

It is worthwhile to mention here that in the present work, one has taken two neutron evaporation on the average. Experimentally it has been observed that on the average ~8 neutrons are evaporated in each decay mode. In this curve, the probability of formation of doubly magic fission fragment ^{132}Sn is quite large, which arises due to restoration of the isospin symmetry. Besides this, some more peaks at remaining shell closure are also seen. This apparently calls for further experiments with refined measurements in the region of mass asymmetry η >0.4. If instead of the cranking masses, we use the average mass parameter (dotted curve), the dip corresponding to fission fragment combination ^{126}Sn +^{128} Sn disappears. Thus the shell effects both in potential and mass parameter play a dominant role in explaining the dips and other structure in the observed data.

IV. CONCLUSION

Through empirical as well as theoretical estimates, one thus conclude that the spin-isospin symmetry plays a dominant role in explaining the fine structure effects in fission fragment mass distribution. A weak strength of *p-n* interaction has direct relevance with the breakdown of spin-isospin symmetry. Restoration of the spin-isospin symmetry at the maxima in *p-n* interaction gives an estimation of number of neutrons evaporated in each decay mode. Here, ATCSM calculations not only reproduce the observed trend nicely but also suggest some new fragments to pop up from the fissioning nucleus ^{254}Fm. These symmetry aspects of fission fragment mass distribution studies are of great significance and therefore, more systematic and refined measurements of the data for larger mass asymmetry (η >0.4) will be of much importance.

ACKNOWLEDGEMENTS

Financial support from the Department of science and Technology, Government of India, is highly acknowledged.

BIBLIOGRAPHY

[1] L. S. Danu et al., Phys. Rev. C **81**, 014311 (2010).
[2] R. Gupta, S. S. Malik and A.K.Jain, in Proceedings of VI International Symposium on Nuclear and Related Techniques XII Workshop on Nuclear Physics WONP-NURT, La Habana, Cuba, 09-12 Feb., 2009, pp.1CD-ROM (InSTEC-CEADEN, Cuba, 2009).
[3] R. Gupta and S. S. Malik, Eur. Phys. J. A **45**, 239 (2010).
[4] R. Gupta and S. S. Malik, J. Phys.: Conf. Ser. **312**, 092028 (2011).
[5] G. Audi, A. H. Wapstra and G. Thibault, Nucl. Phys. A **729**, 337 (2003).
[6] J. -Y. Zhang, R. F. Casten and D. S. Brenner, Phys. Lett. B **227**, 1 (1989).
[7] D. S. Brenner, C. Wesselborg, R. F. Casten, D. D. Warner, J.-Y. Zhang, Phys. Lett. B **243**, 1 (1990).
[8] P. Van Isacker, D. D. Warner and D. S. Brenner, Phys. Rev. Lett. **74**, 4607 (1995).
[9] R. B. Cakirli, EPJ Web Conf. **66**, 01019 (2014).
[10] R. B. Cakirli, D. S. Brenner, R. F. Casten and E. A. Millman, Phys. Rev. Lett. **94**, 092501 (2005).
[11] A. Bohr and B. R. Mottelson, Nuclear Structure, Volume 1 (World Scientific Publishing Co., Singapore, 1998).
[12] P. Singh, H. Kaur and S. S. Malik, Eur. Phys. J. A **50**, 68 (2014).
[13] R. Aroumougame, N. Malhotra, S. S. Malik and R. K. Gupta, Phys. Rev. C **35**, 994 (1987).
[14] J. Maruhn and W. Greiner, Z. Phys. A **251**, 431 (1972).
[15] W. D. Myers and W.J. Swiatecki, Ark. Fys. **36**, 343 (1967).
[16] P. A. Seeger and W. M. Howard, Nucl. Phys. A **238**, 491 (1974).
[17] J. A. Maruhn, W. Greiner and W. Scheid, in Heavy Ion Collisions, Vol. 2 Chap. 6, edited by R. Bock (North Holland, Amsterdam, 1980).
[18] D. R. Inglis, Phys. Rev. **96**, 1059 (1954); S.T. Balyaev, Kgl. Dansk. Vidensk. Sels. Mat.-Fys. Medd. **31**, No.11 (1959).
[19] J. A. Maruhn and W. Greiner, Phys. Rev. Lett. **32**, 548 (1974).
[20] R. K. Gupta, W. Scheid and W. Greiner, Phys. Rev. Lett. **35**, 353 (1975).
[21] O. Zohni, J. A. Maruhn, W. Scheid and W. Greiner, Z. Phys. A **275**, 235 (1975).
[22] F. Caitucoli et al., Radiat. Eff. **92**, 333 (1986).
[23] D. R. Saroha and R.K. Gupta, J. Phys. G: Nucl. Phys. **12**, 1265 (1986).
[24] S. S. Malik, N. Malhotra, D. R. Saroha and R. K. Gupta, International Centre for Theoretical Physics, Trieste, Italy, Report No. IC/86/128 (1986)
[25] S. S. Malik and R. K. Gupta, Phys. Rev. C **39**, 1992 (1989).
[26] K. J. Le Couteur and D.W. Lang, Nucl. Phys. **13**, 32 (1959).
[27] R. Capote et al., Nucl. data sheets **110**, 3107 (2009).
[28] T. von Egidy and D. Bucurescu, Phys. Rev. C **72**, 044311 (2005).
[29] R. A. Senkov and M. Horoi, Phys. Rev. C **82**, 024304 (2010).